International Journal of Solids and Structures 51 (2014) 1066–1074

Contents lists available at ScienceDirect

International Journal of Solids and Structures

journal homepage: www.elsevier.com/locate/ijsolstr

An experimental and numerical investigation of different shear test configurations for sheet metal characterization

Qing Yin [a,*], Benjamin Zillmann [b,*], Sebastian Suttner [c,*], Gregory Gerstein [d], Manfredi Biasutti [c], A.Erman Tekkaya [a], Martin F.-X. Wagner [b], Marion Merklein [c], Mirko Schaper [e], Thorsten Halle [f], Alexander Brosius [g]

[a] Technische Universität Dortmund, Dortmund D-44227, Germany
[b] Technische Universität Chemnitz, Chemnitz D-09125, Germany
[c] Friedrich-Alexander-Universität Erlangen-Nürnberg, Erlangen D-91058, Germany
[d] Leibniz Universität Hannover, Garbsen D-30823, Germany
[e] Universität Paderborn, Paderborn D-33098, Germany
[f] Otto-von-Guericke Universität, Magdeburg D-39104, Germany
[g] Technische Universität Dresden, Dresden D-01069, Germany

ARTICLE INFO

Article history:
Received 4 September 2013
Received in revised form 29 October 2013
Available online 10 December 2013

Keywords:
Simple shear
Heterogeneity
Sheet metal

ABSTRACT

Simple shear tests are widely used for material characterization especially for sheet metals to achieve large deformations without plastic instability. This work describes three different shear tests for sheet metals in order to enhance the knowledge of the material behavior under shear conditions. The test setups are different in terms of the specimen geometry and the fixtures. A shear test setup as proposed by Miyauchi, according to the ASTM standard sample, as well as an in-plane torsion test are compared in this study. A detailed analysis of the experimental strain distribution measured by digital image correlation is discussed for each test. Finite element simulations are carried out to evaluate the effect of specimen geometries on the stress distributions in the shear zones. The experimental macroscopic flow stress vs. strain behavior shows no significant influence of the specimen geometry when similar strain measurements and evaluation schemes are used. Minor differences in terms of the stress distribution in the shear zone can be detected in the numerical results. This work attempts to give a unique overview and a detailed study of the most commonly used shear tests for sheet metal characterization. It also provides information on the applicability of each test for the observation of the material behavior under shear stress with a view to material modeling for finite element simulations.

1. Introduction

During sheet metal forming operations, materials are subjected to high shear stresses (Bae and Ghosh, 2003). Sheet metal characterization under shear loading is therefore an important method to obtain reliable material data for a numerical process design of sheet metal forming operations. Nowadays, the parameters of the needed constitutive laws are determined by standard material characterization methods, such as the standardized uniaxial tensile test. With a view to modern and complex constitutive laws, as for example presented by Barlat et al. (2003) or Banabic (2010), the parameter identification using uniaxial tensile tests is insufficient for their description; further experimental setups generating different load cases need to be considered. In order to identify additional material parameters, many studies of the constitutive behavior during shear deformation, especially for the examination at large strains, were made by Rauch (1992). Bouvier et al. (2006) analyzed the homogeneity of the shear zones depending on the geometric ratio of the shear gauge. They recommended a ratio of 10:1 for the shear bridge length to height in order to maximize the homogeneous part. Kang et al. (2008) compared the results of shear tests to uniaxial tensile results, demonstrating good agreement. The isotropic and kinematic hardening behavior can be observed in cyclic shear tests without changing the testing device or the sample geometry. Various experimental approaches and specimen geometries are suggested in literature. This work presents a comparison of three representative shear test setups: the shear test originally proposed by Miyauchi (1984), the standardized test according to ASTM B831 (ASTM, 2005), and the twin bridge shear test as described in Brosius et al. (2011). We present the experimental analysis of strain distributions and the resulting

* Corresponding authors. Tel.: +49 37153137928 (B. Zillmann).
E-mail addresses: qing.yin@iul.tu-dortmund.de (Q. Yin), benjamin.zillmann@mb.tu-chemnitz.de (B. Zillmann), sebastian.suttner@fau.de (S. Suttner).

0020-7683/$ - see front matter © 2013 Elsevier Ltd. All rights reserved.
http://dx.doi.org/10.1016/j.ijsolstr.2013.12.006

flow curves for an interstitial free steel. Furthermore, we discuss a numerical study of the stress state.

2. State of the art

2.1. Sheet metal characterization

Various testing methods for the characterization of the plastic behavior of sheet materials are established today. Fig. 1 schematically shows some well-known tests and the corresponding stress states in the $\sigma_1 - \sigma_2$ plane. The yield locus can be divided into four quadrants. The first quadrant represents the biaxial tensile stress states, while the third quadrant corresponds to biaxial compression. Shear deformation with one tensile and one compression stress component is located in the second and forth quadrants. The simple tension test can be found on the positive half of the axes. Due to its simplicity and the homogeneous stress and strain distribution, this test is considered as a standard test for many applications. The maximum achievable strain is limited by necking, which occurs for normal sheet metals at an equivalent strain of 0.2–0.3 or even below. On the compression side, the uniaxial compression test bears many difficulties for sheet materials due to their tendency to buckle. This issue is particularly important for applications of cyclic loadings as shown by Cao et al. (2009). Different testing methods are applied to study biaxial tensile stress states: the hydraulic bulge test (Panknin, 1959), the biaxial tensile test (Hannon and Tiernan, 2008) and the stack compression test (Merklein and Kuppert, 2009). Biaxial compression represents the highest difficulty for sheet metal testing. Zillmann et al. (2011) have recently proposed a new test setup using very small quadratic specimens and an optical strain measurement to further analyze this load case.

Shear tests are a convenient way to characterize materials under shear loadings. Hardening curves can be recorded without limitations inherently associated with friction, buckling or necking. Numerous different specimen geometries and testing devices have been proposed for shear testing. Iosipescu (1967) presented a *V*-notched geometry which was further developed and, for example, documented in the ASTM D5379 standard (ASTM, PA). G'Sell et al. (1983) and Rauch and G'Sell (1989) introduced a plane shear test for polymer or metallic sheet materials. This test allows the setting of the principal stress axes in rolling and transverse directions of the sheet. Due to the inhomogeneous strain distribution induced by edge effects, (Bouvier et al., 2006) suggested to increase the ratio of length to width in order to generate a larger central area. Miyauchi (1984) suggested a specimen with two shear gauges and three clamping areas. By a translational movement of the inner area parallel to the outer clamps, both shear gauges are deformed symmetrically, which reduces the rotation moment on the machine. An et al. (2009) compared two Miyauchi-type specimens with rectangular shape and slit shape of the shear zones. For rectangular geometries, the strain distribution is quite homogeneous in the majority of shear length of specimen, while for specimens with slits, the strain distribution is rather inhomogeneous across the larger part of the shear length. The ASTM standard B831–05 (ASTM, 2005) describes a shear specimen that can be directly used in uniaxial testing machines because of its simple geometry. Diagonal slits are arranged on a sheet strip so that a small zone is sheared when tensile loads are applied. Shouler and Allwood (2010) also studied the fomability of sheet materials using shear specimens. While shear tests are commonly conducted using a translational displacement, torsion also leads to simple shear deformation. Marciniak (1961) proposed the in-plane torsion test for sheet metal testing, which was further developed by Pöhlandt and Tekkaya (1985) and Bauer (1989). Recently, a shear test using the in-plane torsion kinematics was also suggested by Brosius et al. (2011): the so-called twin bridge shear test. In the remainder of this paper, we focus on three approaches for shear testing: the Miyauchi shear test, the shear test according to ASTM B831 and the twin bridge shear test using in-plane torsion.

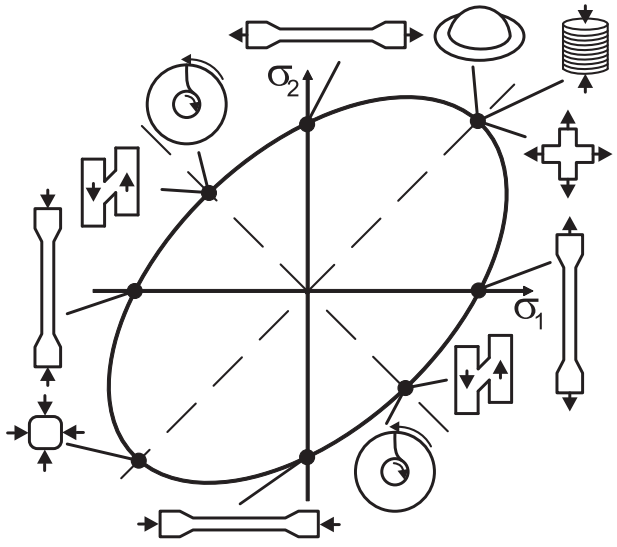

Fig. 1. Overview of testing methods for sheet metal characterization.

2.2. Miyauchi shear test

Miyauchi (1984) proposed a simple shear test with two shear zones, Fig. 2. The specimen has three bars that are all clamped, and that are connected by the regions that represent the two shear zones. When a tensile load is applied to the middle bar, the connecting regions will be deformed by shear deformation. This geometry reduces the rotation of the shear zone during loading. However, while this approach provides a work-around for the rotation of the shear direction, it creates a different rotation of the principal stress directions in the two shear zones during deformation. As a consequence, an anisotropic material response may be partially averaged out and may probably not be fully represented by the experimental data. The slits in the specimen help to reduce the premature failure due to stress concentrations on the edges. The geometry of the specimen, especially the length of the shear zone, can affect the measured work hardening, as investigated by An et al. (2009), where two different geometries were used. An et al. (2009) recommended the rectangular specimen since the strain distribution in the shear zone is quite homogeneous. The

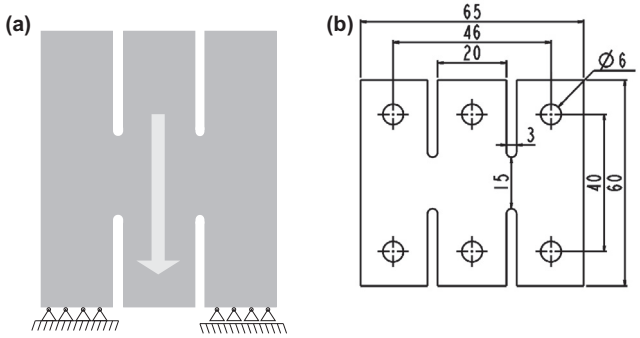

Fig. 2. Schematic representation of the (a) Miyauchi test setup and (b) specimen geometry proposed by Zillmann et al. (2012). The arrow indicates the direction of force.

study by An et al. (2009) also shows that plastic anisotropy has a minor effect on the measured shear stresses. Moreover, it was found that the strain distribution in the shear zone has a pronounced effect on the measured work hardening. Therefore, special care must be taken to use well adapted strain measurement methods during the test. Further detailed studies on the effect of different Miyauchi specimen geometries on experimental flow curves can be found in, e.g., van Riel and van den Boogaard (2007); Merklein and Biasutti (2011); Zillmann et al. (2012).

2.3. Shear test according to ASTM B831

A well-known test setup for simple shear tests of thin wrought sheet metals is based on the American Society for Testing and Materials standard ASTM B831 (ASTM, 2005). The ASTM standard for single shear testing was developed primarily to investigate the behavior of thin aluminum products under shear loading using a single shear zone. This leads to a simple geometry (Fig. 3(a)) and a simple evaluation of shear stresses and strains. The planar simple shear test with a single shear zone is a very efficient technique to evaluate the mechanical properties of flat samples and to analyze the in-plane plastic anisotropy of metals (Rauch, 1998). Because of the single shear zone, the anisotropic material response can be studied in greater detail comparison to the Miyauchi type specimen. The original ASTM sample is used in a tension testing machine, where the shear stress is calculated from the uniaxial tensile force. This planar simple shear experimental setup can be realized on a universal testing machine with a built-in fixture device, as, for example, developed by Staud and Merklein (2009). The uniaxial load of the machine enforces a parallel movement of two lateral grips (Bouvier et al., 2006). However, the specimen rotates during testing. This rotation can be reduced by a very stiff clamping tool and by using an adequate clamping force, but a strong clamping force can damage the specimen or result in an undesirable deformation when the fixture device is not fully aligned in the same plane as the specimen. A displacement of the upper and lower tool out of this plane leads to a warping of the specimen that can cause premature failure of the shear specimen. This can be avoided by an adequate positioning of the tool in the testing machine with low tolerances. A modified simple shear specimen (Fig. 3(b)) based on the ASTM standard was developed by Merklein and Biasutti (2011) to facilitate a reversal of the load direction. This opens a pathway to evaluate the material behavior under cyclic shear loading to describe kinematic hardening behavior.

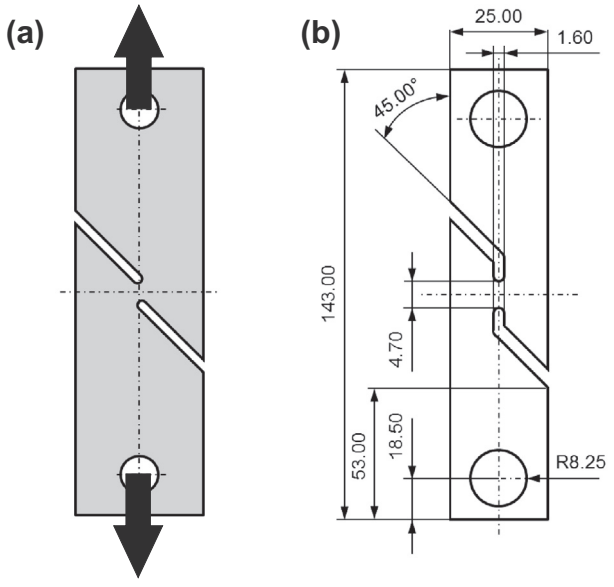

Fig. 3. Simple shear test specimen according to (a) ASTM B831–05 standard and (b) a modified ASTM specimen proposed by Merklein and Biasutti (2011). The arrows indicate the direction of force.

2.4. Twin bridge shear test

The twin bridge shear test is a variant of the in-plane torsion test originally introduced by Marciniak (1961). A round sheet specimen is clamped concentrically in the center and on its outer rim. By a relative rotation between inner and outer fixtures, shear deformation takes place in the annular area in-between. Compared to other shear tests, the loading is applied as a moment instead of a force couple. Therefore, no additional unwanted reaction moment is created which has to be compensated by the clamps. Brosius et al. (2011) presented a modified geometry with two slits in the round sheet specimen, creating two shear zones where the deformation is localized (Fig. 4). The bridge dimensions are defined by the radius r_m, the height Δr, and the arc length ϑ. By twisting the clamps, both bridges are deformed in the same orientation. This modified specimen geometry exhibits completely different characteristics than the original in-plane torsion test without slits. While the original in-plane torsion test is able to generate a shear stress state without edge effects, the twin bridge specimen is suitable to determine shear curves for anisotropic materials. Yin et al. (2012) presented a method based on the modified geometry to identify kinematic hardening parameters using an inverse approach without stress measurements.

3. Experimental procedure

3.1. Material

The tested material DC06 is an interstitial free steel which belongs to the category of cold-rolled low carbon steel. The material batch was delivered by ThyssenKrupp Steel Europe. After cold rolling, the material was annealed and subjected to the final skin-pass by the manufacturer. The sheet thickness is 1 mm. The average yield strength in uniaxial tension and the Lankford coefficients for $0^\circ, 45^\circ$ and 90° with respect to the rolling direction is given in Table 1. All test specimens used in this work were prepared from the same batch. More detailed information about this material batch regarding the initial texture, grain size etc., is given in Clausmeyer et al. (2012). The tested direction in the presented study is 45° with respect to the rolling direction.

3.2. Strain measurements and strain calculations

A consistent measurement technique of the shear strain was defined to compare the different shear tests. In all cases, the strain

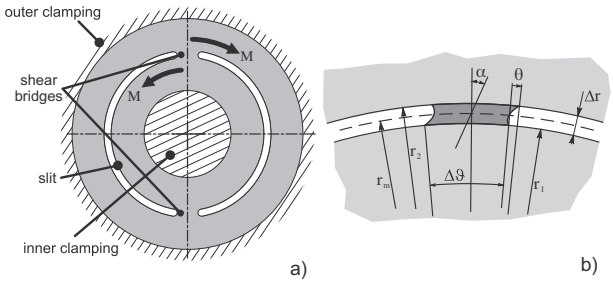

Fig. 4. In-plane torsion test according to Brosius et al. (2011) (a) twin bridge specimen; (b) geometry of the shear zone.

Table 1
Mechanical properties in uniaxial tension with respect to the rolling direction.

Angle to rolling direction	$\sigma_{0.2}$ (MPa)	r-value
0°	141	2.3
45°	142	1.9
90°	142	2.8

distributions in the shear zones were measured with a digital imaging correlation (DIC) system. Strains were analyzed by taking the average strain value along the longitudinal direction, as shown in Fig. 5. Moreover, to characterize homogeneity of the strain distributions, strains were also analyzed along the transversal direction. For each time step, the average strain value along the longitudinal direction (which is located in the middle of the shear zone) was selected as representative measure for the macroscopic shear strain:

$$\gamma_{meas} = \frac{1}{l}\int_{x=0}^{x=l} \gamma(x)dx. \quad (1)$$

where l is the length of the evaluated region.

3.3. Miyauchi test

In the present study, the modified Miyauchi specimen proposed by Zillmann et al. was used (see also Fig. 2(b)). The width to thickness ratio is 3 : 1 and the ratio of length to width is 5 : 1. The fixture used in the experiments (Fig. 6) clamps the specimen on the three bars (using juck chaws) in direction of the sheet thickness. The design of the fixture allows direct observation of the specimen surface to determine surface strains in the shear zones using the DIC method. The machine speed was set to 0.3 mm/min which leads to a shear strain rate of 0.001 s^1. The shear stress τ can be determined as

$$\tau = \frac{F}{2 \cdot l_0 \cdot s_0} \quad (2)$$

where F is the force required to deform the two shear zones and l_0 and s_0 represent the initial gauge length and the initial sheet thickness, respectively.

3.4. ASTM B831

A universal tensile machine was used for the simple shear tests with a built-in fixture that consists of two hydraulic clamps, Fig. 7.

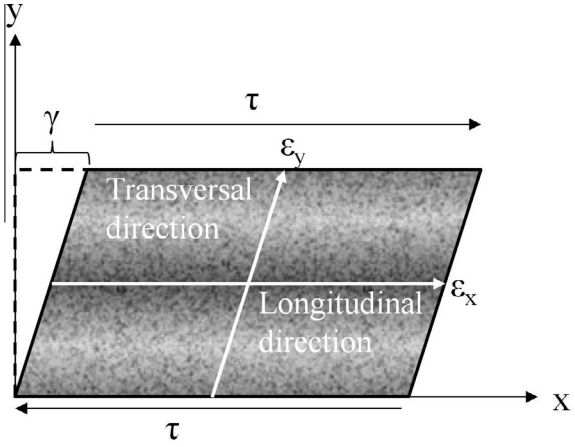

Fig. 5. Analysis of the strain distribution is demonstrated by two different directions.

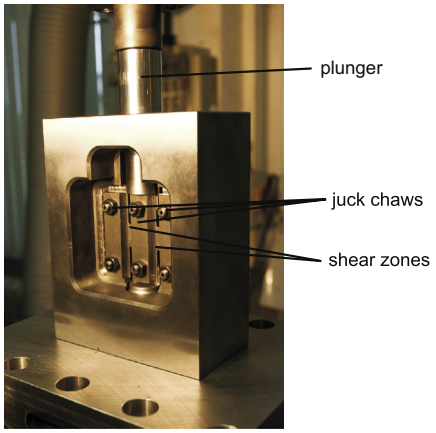

Fig. 6. Fixture that was used for the modified Miyauchi specimen.

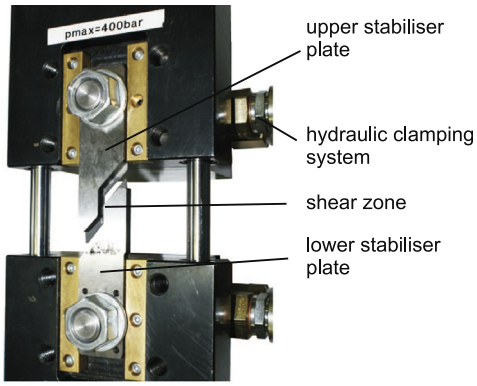

Fig. 7. Fixture (built in tool) for the modified ASTM specimen.

To suppress rotation of the specimen, two stabilizer plates are installed on the upper and lower clamping tool. The shear zone of the specimen is not covered by the plates. On the upper clamping device, a load cell is mounted to measure the uniaxial force for determining the shear stress during the movement of the crosshead. The crosshead motion was adjusted at a constant machine speed of 0.1 mm/min which leads to a shear strain rate of 0.001 s^1. The geometry used in this study is a modified ASTM B831–05 standard test geometry developed by Merklein and Biasutti (2011). The shearing zone of the specimen has an initial length of $l_0 = 4.7$ mm and a width of $b_0 = 1.6$ mm (see also Fig. 3(b)), which corresponds to a length to width ratio of 2.9 : 1 and a width to thickness ratio of 1.6 : 1. The shear stress τ can be determined from

$$\tau = \frac{F}{l_0 \cdot s_0}. \quad (3)$$

3.5. Twin bridge shear test

The torsion testing on the twin bridge specimen was conducted using the device described by Yin et al. (2011), Fig. 8. Integrated in a universal testing machine, an inner clamping force of up to 50 kN can be applied. The rotation of the outer fixtures is provided by a servo motor using a worm gear. Sensors measure torque and rotation angle during testing, and strains can again be documented by DIC. The dimensions of the specimen's slits are listed in Table 2. The twin bridge specimen has an outer radius of 40 mm. Since the outer clamping radius is 30 mm, an annular area of 10 mm width is fixed under the clamping ring. The inner clamping radius

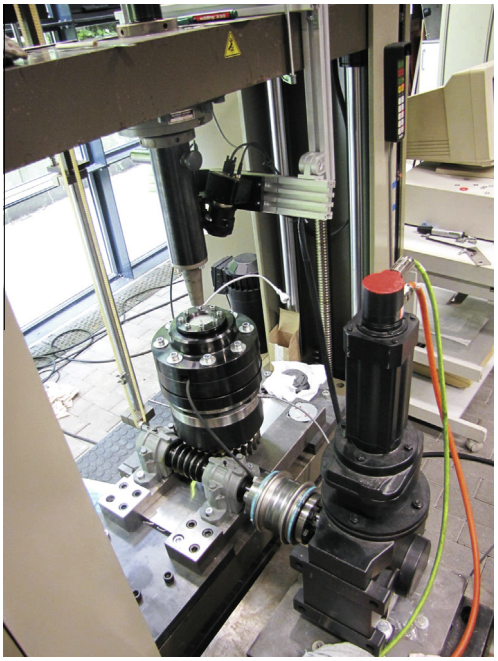

Fig. 8. Experimental setup for in-plane torsion testing used for the twin bridge specimen.

Table 2
Dimensions of the twin bridge specimen.

Specimen radius	40 mm
r_i	15 mm
r_0	30 mm
$\Delta\vartheta$	20°
r_m	21.5 mm
Δr	1 mm
r_1	21 mm
r_2	22 mm
r_s	0.5 mm

is 15 mm. The dimension of the shear bridges is defined by the slit geometry. In the present configuration the shear zone height is 1 mm and the length is about 7.5 mm which leads to a length to width ratio of 7.5 : 1. Compared to the initially presented shear zone shape of Brosius et al. (2011), notch radii of r_s are applied in order to avoid premature cracks at the corners (Fig. 4(b)). The shear stress can be calculated by

$$\tau = \frac{M}{s_0 \cdot \Delta\vartheta \cdot r_m^2} \tag{4}$$

using the applied torque M. As shown in Brosius et al. (2011), the theoretical strain calculation

$$\gamma = \tan\alpha = \frac{\theta \cdot r_m}{\Delta r} \tag{5}$$

cannot be directly applied due to the outspread of plastic deformation to adjacent areas. Therefore, optical strain measurements are required also in this test in order to determine the strains in the shear bridges.

4. Results and discussion

4.1. Experimental strain distributions and flow curves

The strain distributions are now discussed along the two different directions in the shear zones (see Fig. 5). The homogeneity of the shear zone is discussed for total equivalent strains (including elastic strains) of 0.05 and 0.2. The equivalent v. Mises strain ε_{eq} was calculated for each time step along the longitudinal direction, using the surface strain components obtained from the DIC measurements. The major and minor strains along the longitudinal and transversal directions for each specimen type are presented in Fig. 9. Generally, strains are lower near the center of the shear zone. In longitudinal direction, strains rapidly increase from the edges and reach a maximum at a relative distance of about 0.1 (Fig. 5(a)). Strain inhomogeneity increases with higher deformations. The distributions of the two principal strains are very similar for all specimen geometries and test setups. There are some minor differences near the edges in the longitudinal direction between the specimens, that can most likely be related to the different height to width ratios of the shear zones. The major and minor strain in the center of the shear zone is identical in transversal and longitudinal direction, which indicates that the specimens produce a shear deformation that is very close to the ideal case. As an example, the measured strain distributions for an average equivalent plastic strain of 0.2 along the longitudinal direction are shown in Fig. 10. Although variations in strains (related to the different designs of the shear zones) are clearly visible in all samples, the differences are low for the plotted equivalent strain and all samples can be used to study quite homogeneous shear deformation.

The experimental shear stress vs. shear strain curves determined with the different specimen types are shown in Fig. 11. It can be clearly seen that the curves exhibit a similar hardening behavior and are generally in excellent agreement up to shear strains of 0.8. Small deviations of the curves can occur because of material inhomogeneity, e.g. thickness variations. A divergence is seen at large strains of more than 0.8 which can be a result of necking.

4.2. Numerical results

In order to further evaluate the local and overall response of the different shear specimens considering both strains and stresses, finite element simulations were conducted. The shear specimens were meshed with 2D plane stress elements (CPS3 and CPS4R) in ABAQUS/Standard. The element edge length in the shear zone was set to 0.1 mm. Isotropic elastic–plastic material behavior according to von Mises was used in the simulation. The non linear geometric option (nlgeom) is used. The flow curve used for the input of the numerical simulation was extrapolated from the result of a uniaxial tensile test in RD of this material. The extrapolation approach of Swift was used. Specimen dimensions used in the simulation correspond to the experimental setups described in the previous sections. The loading was realized in all tests by applying a boundary condition as a translational displacement or a rotation on the clamped nodes, following the real experimental kinematics. Stresses and strains were analyzed along the same (longitudinal and transversal) directions described above. Corresponding to the experimentally determined shear curves using optical strain measurements, a similar approach was used in order to evaluate the ability of the shear tests to reproduce a given hardening curve. For this purpose, the strain of the flow curve is calculated from the average value along the longitudinal section cut. The stresses are not taken from the elemental results of the simulation, but are determined from Eqs. (2)–(4) using the reaction moment or reaction force data in the history output of the simulations. The calculation of the stress vs. strain curves in the simulations therefore correspond closely to the real experiments.

Fig. 12 shows the simulated flow curves that represent the response of each specimen to a well-defined input flow curve in a purely numerical analysis. All three tests are able to reproduce the given flow curve with good accuracy up to an equivalent plastic

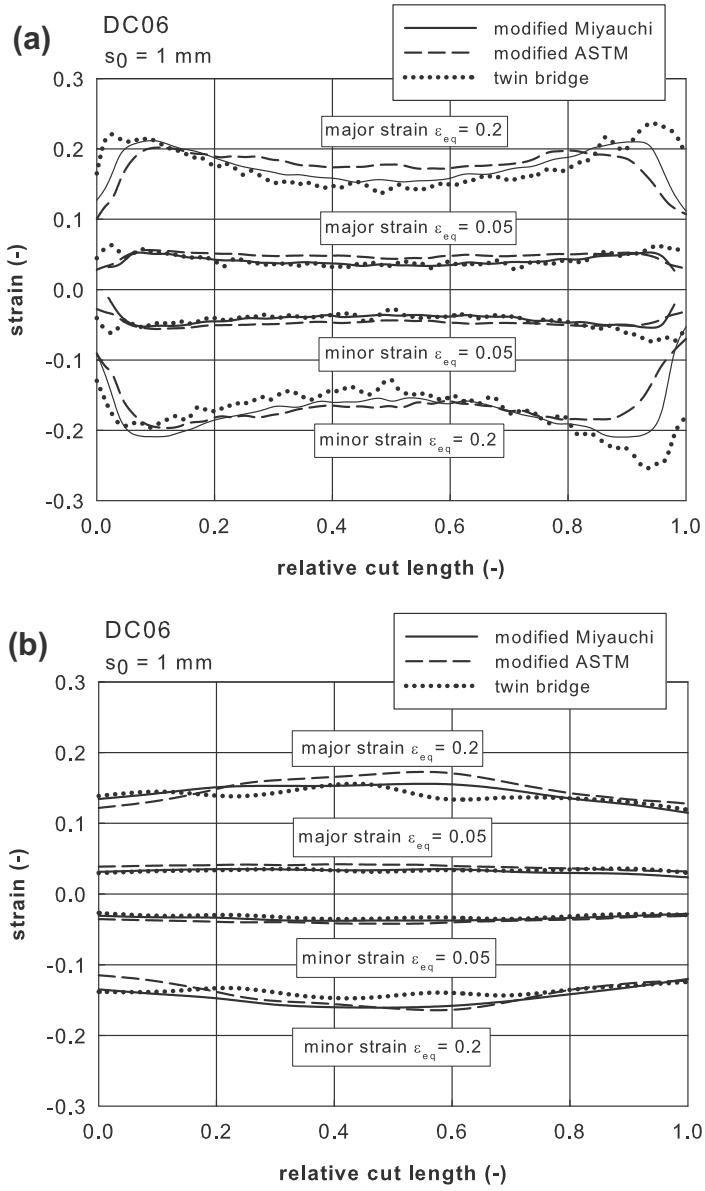

Fig. 9. Experimental strain distribution along the (a) longitudinal and (b) transversal direction of the shear zone for the three specimens determined with the software Aramis. The plots are generated at an average equivalent v. Mises strain ε_{eq} of 0.05 and 0.2 along the longitudinal direction.

strain of 0.3. With higher strains, all specimens tend to overestimate the flow curve. However, all three tests fulfill the requirement of reproducing the original hardening behavior, since the error at larger strains is the result of severely distorted elements at the edges. At this stage of deformation, the simulation is not capable of describing the specimen behavior anymore, since crack initiation at the edges and the development of fracture is not considered in the used material model. Thus, these numerically obtained shear flow curves do not provide information about the achievable strain in the shear tests. In a further step, the distributions of the numerically calculated shear stresses along the longitudinal and transversal cuts are compared for a shear strain of 0.4, which is equal to an equivalent plastic strain of about 0.23. The analysis of the stresses are resolved in the global coordinate system. The results are shown in Fig. 13. Since the absolute cut length varies for all geometries, the relative cut length is used for comparison. Along the longitudinal direction, shear stress distributions for all three specimens exhibit a maximum next to the edges. The position of this maximum is different due to the aspect ratios of shear zone width and height. In the center, the same value can be obtained for all three tests. In the transversal direction, shear stresses decrease with increasing distance from the center. The results for the Miyauchi and the twin bridge specimen agree more closely than the results for the modified ASTM shear test. Qualitatively, the distribution of shear stresses is comparable for all three tests.

For a more detailed analysis of the stress state, the normal stress components σ_x in longitudinal and σ_y in transversal direction are shown in the diagrams of Fig. 15. The Miyauchi and the modified ASTM shear test reach a σ_x value of 40–50 MPa, which is the tensile component of the stress tensor parallel to the shear direction. For the twin bridge specimen, this component is also a tensile stress with high values near the edges and a minimum near the center of about 9 MPa. The stress component σ_y is also positive for the Miyauchi and the modified ASTM specimen, thus much smaller than σ_x. A different distribution occurs for σ_y in the twin bridge specimen, which changes from tensile to compressive stresses along the longitudinal cut. Some remarks have to be made with respect to the stress analysis. Since there are tensile stress components at the edges of the shear zone, necking can occur during

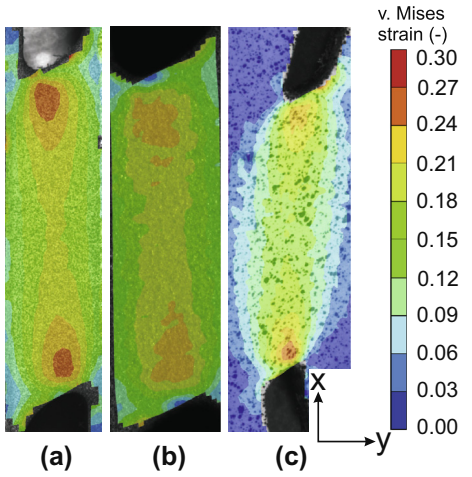

Fig. 10. Experimental v. Mises strain determined with the software Aramis at an equivalent strain of 0.2 which is the average value in the longitudinal direction in the center of the shear zone for (a) modified Miyauchi (b) modified ASTM (c) twin bridge specimen.

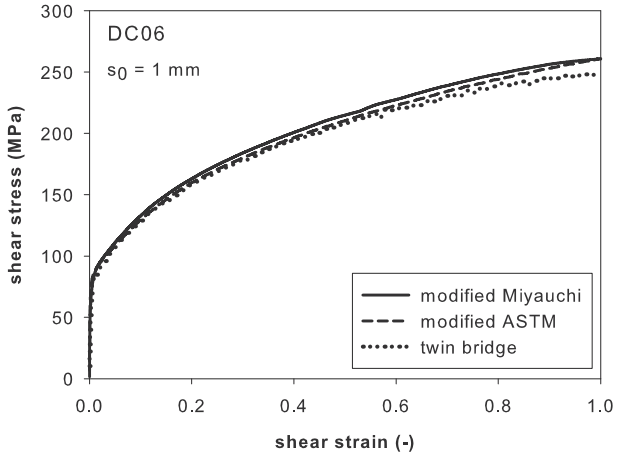

Fig. 11. Experimental shear stress vs. shear strain curves for three shear test setups.

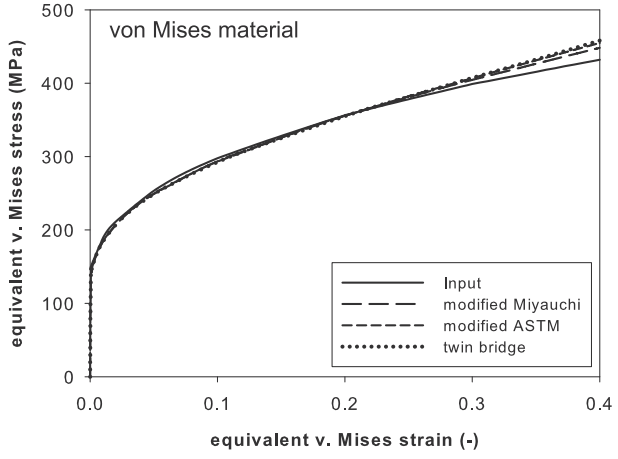

Fig. 12. v. Mises shear stress vs. strain curves gained from the simulation for three shear test setups.

deformation. This again can change the material thickness which is neglected for the stress calculation in the experiment and the 2D numerical study. The Miyauchi setup was exemplarily modeled

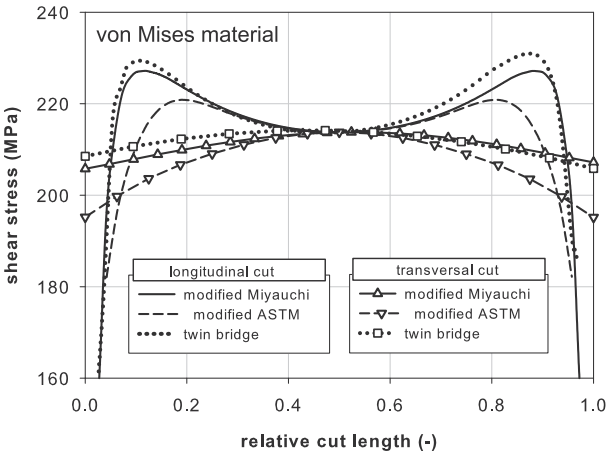

Fig. 13. Shear stress distribution for the longitudinal and transversal cut gained from the simulation at an average equivalent strain of 0.23 in the longitudinal direction.

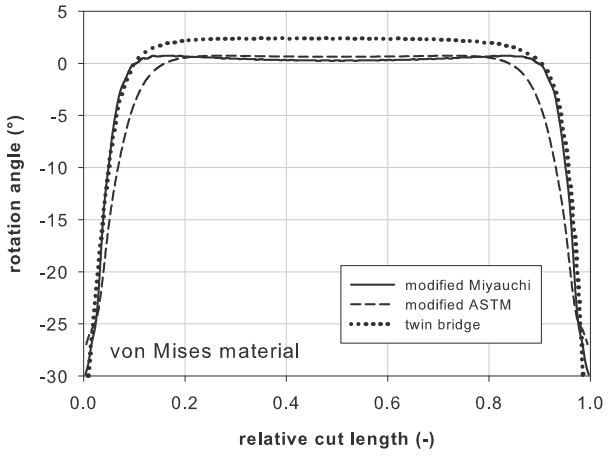

Fig. 14. Rotation angle in longitudinal direction gained from the simulation at an average equivalent strain of 0.23 in the longitudinal direction.

in 3D with three elements in the thickness direction to capture the change in thickness. At an average shear strain of 0.4 in the longitudinal direction, a thickness reduction of less than 1% in the middle of the shear zone and smaller than 6% on the edges was detected. The stress vs. strain curve was calculated with the same method as used in the 2D simulation and compared to each other. The 2D and 3D results are identical in their stress vs. strain response. Thus, the change of thickness for the shown shear specimens is negligible. Another aspect to validate the specimen geometries is the rotation of the shear zone during deformation. A high rotation during shearing would change the loading direction and the anisotropy is smeared out. Fig. 14 shows the rotation angle at an average equivalent strain of 0.23 in the longitudinal direction for the three setups. At both ends, a rotation angle of about 30° can be found for the analyzed shear specimen. However, the central area is not affected by the rotation. For the Miyauchi and the ASTM specimen, a rotation angle of about 0.5° was calculated. The distant clamping situation in the twin bridge specimen causes slightly higher rotation (2.5°) of the central shear zone area. Comparing the rotated areas to the unrotated region, about 10% of the shear zone length at each length scale is significantly affected by the edge rotation. The ASTM specimen shows a smaller ratio of shear zone length to height compared to the Miyauchi specimen. Therefore, the large edge rotation affects a higher amount of the shear

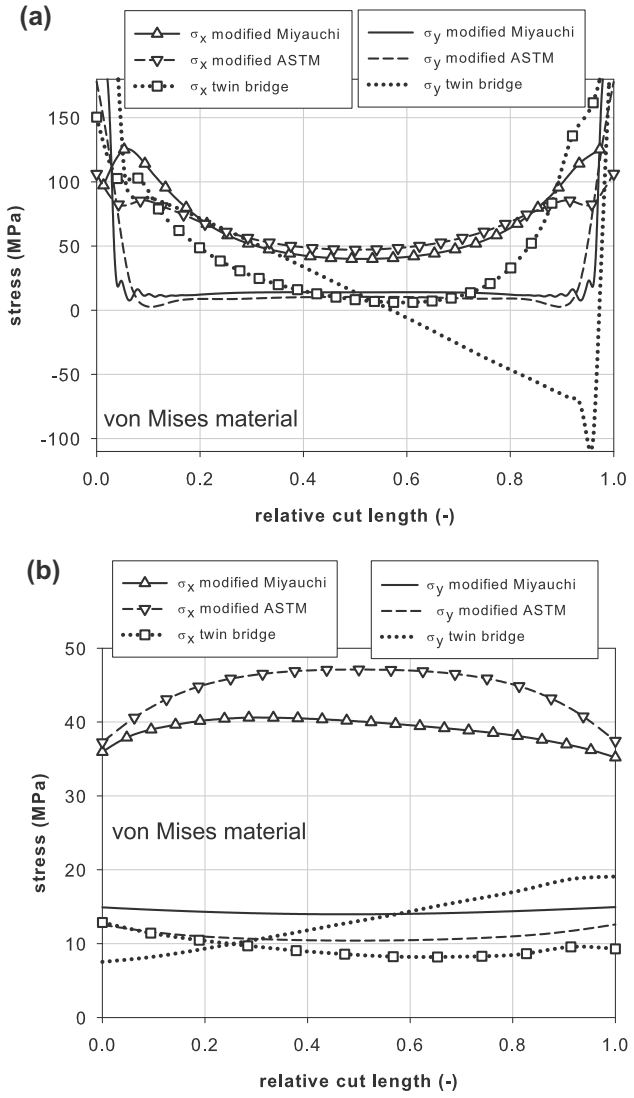

Fig. 15. Stress components in x and y direction gained by the simulation at an average equivalent strain of 0.23 in the longitudinal direction, where the x direction is parallel to the shear direction. (a) Longitudinal cut and (b) transversal cut.

zone. Considering the experimental results, a good accordance can be found despite these differences. The major part of the shear zone remains almost unrotated. The rotation near the edges can be neglected during the evaluation.

To summarize the numerical results, the chosen method to estimate the macroscopic shear strain as an average along a longitudinal cut through the center of the shear zone is applicable for all three shear tests. However, different stress distributions occur, especially for the normal stress components in x and y-direction. All three test setups only represent an approximation of simple shear deformation even in the center of the shear zones. While the different specimens are characterized by different stress states, the numerically determined flow curves are in good agreement with the given curve. The normal stresses and their varying distribution obviously only have a minor influence on the overall estimation on shear strains.

5. Summary and conclusions

In this study, three different shear test setups using different specimen geometries were compared based on experimental data and numerical simulations. Specimen geometries were varied with a special focus on the size of the shear zones and their length to width ratios (varied from 2.9: 1 to 7.5: 1). Moreover, different specimen/ fixture designs required different methods of force application. The experimental results show that shear stress vs. shear strain curves obtained from the different test setups are in a good agreement, provided that strains are measured using a digital image correlation system. This method has the additional advantage of providing detailed information on local strain distributions in the shear zones, which were found to also be quite similar in all specimen types studied here.

The results of finite element simulations of the different shear tests also demonstrate that the stress vs. strain curves can be directly compared when the strain analysis is designed to fully mimic the experimental approach. Moreover, the finite element simulations allow for a careful analysis of the local stresses and reveal some minor differences in terms of the stress distribution. In particular, the distribution of shear stresses along the longitudinal axis is generally not homogeneous, except near the center of the shear zones. In addition, relatively small uniaxial tensile stresses occur parallel to the shear direction.

The combined experimental and numerical work presented here suggests that the shear zone length to width ratio only has a minor effect on the strain distribution in the shear zones; the small rotation of the principal stress directions that occurs in the Miyauchi specimen also hardly affects the measured work hardening. The macroscopic mechanical behavior (as represented by the work hardening) of sheet metals under simple shear loading can therefore be documented accurately, irrespective of which specimen geometry is used, if an optical strain measurement system is used.

Acknowledgment

The authors gratefully acknowledge funding by the German Research Foundation (Deutsche Forschungsgemeinschaft, DFG) through Project PAK 250.

References

An, Y.G., Vegter, H., Heijne, J., 2009. Development of simple shear test for the measurement of work hardening. J. Mater. Process. Technol. 209, 4248–4254.
ASTM, PA. ASTM D5379/ D5379M–05 Standard test method for shear properties of composite materials by the V-notched beam method, West Conshohocken.
ASTM, 2005. Test method for shear testing of thin aluminum alloy products. ASTM Int.
Bae, D.H., Ghosh, A.K., 2003. A planar simple shear test and flow behavior in a superplastic Al–Mg alloy. Metall. Mater. Trans. A 34, 2465–2471.
Banabic, D., 2010. Sheet Metal Forming Processes. Springer.
Barlat, F., Brem, J.C., Yoon, J.W., Chung, K., Dick, R.E., Lege, D.J., Pourboghrat, F., Choi, S.H., Chu, E., 2003. Plane stress yield function for aluminum alloy sheets-part 1: theory. Int. J. Plast. 19, 1297–1319.
Bauer, M., 1989. Ermittlung der Fliesskurven von Feinblechen im ebenen Torsionsversuch (Dissertation). University of Stuttgart.
Bouvier, S., Haddadi, H., Levée, P., Teodosiu, C., 2006. Simple shear tests: experimental techniques and characterization of the plastic anisotropy of rolled sheets at large strains. J. Mater. Process. Technol. 172, 96–103.
Brosius, A., Yin, Q., Güner, A., Tekkaya, A.E., 2011. A new shear test for sheet metal characterization. Steel Res. Int. 82, 323–328.
Cao, J., Lee, W., Cheng, H.S., Seniw, M., Wang, H.P., Chung, K., 2009. Experimental and numerical investigation of combined isotropic-kinematic hardening behavior of sheet metals. Int. J. Plast. 25, 942–972.
Clausmeyer, T., Gerstein, G., Bargmann, S., Svendsen, B., van den Boogaard, A.H., Zillmann, B., 2012. Experimental characterization of microstructure development during loading path changes in bcc sheet steels. J. Mater. Sci. 48, 674–689.
G'Sell, C., Boni, S., Shrivastava, S., 1983. Application of the plane simple shear test for determination of the plastic behaviour of solid polymers at large strains. J. Mater. Sci. 18, 903–918.
Hannon, A., Tiernan, P., 2008. A review of planar biaxial tensile test systems for sheet metal. J. Mater. Process. Technol. 198, 1–13.
Iosipescu, N., 1967. New accurate procedure for single shear testing of metals. J. Mater. 2, 537–566.

Kang, J., Wilkinson, D.S., Wu, P.D., Bruhis, M., Jain, M., Embury, J.D., Mishra, R.K., 2008. Constitutive behavior of AA5754 sheet materials at large strains. J. Eng. Mater. Technol. 130.

Marciniak, Z., 1961. Influence of the sign change of the load on the strain hardening curve of a copper test subject to torsion. Arch. Mech. Stosowanj 13, 743–751.

Merklein, M., Biasutti, M., 2011. Forward and reverse simple shear test experiments for material modeling in forming simulations. In: Hirt, G., Tekkaya, A.E. (Eds.), International Conference on Technology of Plasticity, Aachen. pp. 702–707.

Merklein, M., Kuppert, A., 2009. A method for the layer compression test considering the anisotropic material behavior. Int. J. Mater. Form. 2, 483–486.

Miyauchi, K., 1984. A proposal of a planar simple shear test in sheet metals. Sci. Pap. Inst. Phys. Chem. Res. (Jpn.) 78, 27–40.

Panknin, W., 1959. Der hydraulische Tiefungsversuch und die Ermittlung von Fliekurven (Dissertation). University of Stuttgart.

Pöhlandt, K., Tekkaya, A.E., 1985. Torsion testing – plastic deformation to high strains and strain rates. Mater. Sci. Technol. 1, 972–977.

Rauch, E.F., 1992. The flow law of mild steel under monotonic or complex strain path. Solid State Phenom. 23–24, 317–333.

Rauch, E.F., 1998. Plastic anisotropy of sheet metals determined by simple shear tests. Mater. Sci. Eng. A 241, 179–183.

Rauch, E.F., G'Sell, C., 1989. Flow localization induced by a change in strain path in mild steel. Mater. Sci. Eng. A 111, 71–80.

Shouler, D.R., Allwood, J.M., 2010. Design and use of a novel sample design for formability testing in pure shear. J. Mater. Process. Technol. 210, 1304–1313.

Staud, D., Merklein, M., 2009. In: Borsutzki, M., Geisler, S. (Eds.), Zug-Druck-Versuche an Miniaturproben zur Erfassung von Parametern für kinematische Verfestigungsmodelle. Tagungsband Werkstoffprüfung, Düsseldorf, pp. 211–218.

van Riel, M., van den Boogaard, A.H., 2007. Stress–strain responses for continuous orthogonal strain path changes with increasing sharpness. Scr. Mater. 57, 381–384.

Yin, Q., Brosius, A., Tekkaya, A.E., 2011. Modified plane torsion tests for sheet metal characterization. In: Hirt, G., Tekkaya, A.E. (Eds.), International Conference on Technology of Plasticity, Aachen. pp. 696–701.

Yin, Q., Soyarslan, C., Güner, A., Brosius, A., Tekkaya, A.E., 2012. A cyclic twin bridge shear test for the identification of kinematic hardening parameters. Int. J. Mech. Sci. 59, 31–43.

Zillmann, B., Härtel, M., Halle, T., Lampke, T., Wagner, M.F.-X., 2011. Automotive aluminum sheets during in-plane uniaxial and biaxial compression loading. In: Hirt, G., Tekkaya, A.E. (Eds.), International Conference on Technology of Plasticity, Aachen. pp. 691–695.

Zillmann, B., Clausmeyer, T., Bargmann, S., Lampke, T., Halle, T., Wagner, M.F.-X., 2012. Validation of simple shear tests for parameter identification considering the evolution of plastic anisotropy. Tech. Mech. 32, 622–630.